



Received on 19 November 2019; received in revised form, 26 December 2019; accepted, 28 December 2019; published 01 January 2020

PHYTOCHEMICAL SCREENING, SILVER NANOPARTICLE SYNTHESIS AND ANTIBACTERIAL STUDIES ON THE LEAVES OF *AESCHYNOMENE ASPERA* L.

Kataru Vishnuvardhan¹, Kavitha Bommana² and Yasodamma Nimmanapalli^{*1}

Department of Botany¹, Sri Venkateswara University, Tirupati - 517501, Andhra Pradesh, India.

Rayalaseema University², Kurnool - 518002, Andhra Pradesh, India.

Keywords:

Aeschynomene aspera,
Nanoparticles, Green synthesis,
Antioxidant, Antibacterial activity

Correspondence to Author:

Dr. N. Yasodamma

Professor,
Department of Botany,
Sri Venkateswara University,
Tirupati - 517501, Andhra Pradesh,
India.

E-mail: yasodanpalli@gmail.com

ABSTRACT: Green synthesis is one of the best routes for the silver nanoparticles (AgNPs). The present study revealed that the aqueous leaf extracts of *Aeschynomene aspera*, which contains alkaloids, flavonoids, phenols, terpenoids, anthocyanidins, indoles, glycosides, saponins and tannins, is found to be responsible for bioreduction during the synthesis of silver nanoparticles (SNPs). The colour change from light yellow to dark brown within 20 to 60 min indicates the formation of nanoparticles. The UV-Visible spectrum of the aqueous medium containing silver nanoparticles showed a Surface Plasmon Resonance peak at 450 nm. FT-IR analysis reveals that the phenols and amides are mainly responsible for reduction. XRD analysis clearly showed the characteristic Bragg peaks of (111), (200), (220), (311) facets of the face-centered cubic structure of silver nanoparticles and confirmed that these nanoparticles are crystalline in nature. HR-TEM analysis revealed that the green synthesized SNPs were spherical in shape with an average size of 10 nm. The antibacterial effect of synthesized AgNPs on different bacterial strains with the zone of inhibition 14.1 mm on *Escherichia coli* 12.2 mm on *Pseudomonas aeruginosa*, 11.3 mm on *Staphylococcus aureus* and 11.1 mm on *Bacillus subtilis* respectively. DPPH analysis shows that the nanoparticles possess 67.48 percent of antioxidant activity. The above results also correlated with the other species of Fabaceae such as, *Abrus precatorius*, *Cicer arietinum*, *Callindra haematocephala* *Clitoria ternatea*, and *Pongamia pinnata* both in their nanoparticles characteristics and also their antibacterial activity.

INTRODUCTION: Synthesis of silver nanoparticles with the plant extracts is the most implemented method of green and eco-friendly fabrication. Silver nanoparticles are widely used because of their unique properties and promising applications as anticancer and antimicrobial agents^{1,2,3}.

As plants are extensively distributed, easily accessible, safe to handle and possess therapeutically important metabolites it is worthwhile to employ nanoparticle synthesis for numerous applications.

Several plants from Fabaceae family have several bioactive compounds having ethnomedicinal values. The examples of Fabaceae family members exhibiting therapeutic values comprise *Baphia racemosa*, *Crotalaria capensis*, *Dalbergia nitidula*, *Erythrina caffra*, *Indigofera cylindrical*, *Lonchocarpus nelsii*, *Podalyria calyprate*, *Virgilia divaricata*, *Xyliatorreana* (antibacterial, antioxidant and cytotoxic)⁴, *Cicer arietinum*⁵ and *Abrus*

<p>QUICK RESPONSE CODE</p> 	<p>DOI: 10.13040/IJPSR.0975-8232.11(1).451-63</p>
<p>This article can be accessed online on www.ijpsr.com</p>	
<p>DOI link: http://dx.doi.org/10.13040/IJPSR.0975-8232.11(1).451-63</p>	

precatorius (exhibit purgative, emetic, toxic, anti-phlogistic, aphrodisiac and ophthalmic activities). Hot water extracts of dried leaves and roots are applied to treat eye diseases, and are orally consumed to treat nervous weakness ⁶, *C. ternatea* used as memory enhancer, antistress, anxiolytic, antidepressant, anticonvulsant, tranquilizing and sedative agent ⁷, *Calliandra haematocephala* is an ornamental tree with traditional medicinal values consisting large amount of amino acids shows resistance towards fungal organisms. Presence of pipercolic acid, *trans-4* and *trans-5*-hydroxy-pipercolic acid, *trans-cis-4*, 5-dihydroxy-pipercolic acid is reported ⁸. The bioactive compounds from the Fabaceae members are being currently

investigated for their role in the synthesis of nanoparticles. Other members of Fabaceae family possessing medicinal values include *Pongamia pinnata*, used as antiseptic, blood purifier and wound healing agent. This plant also possess antioxidant, antiproliferative, anti-inflammatory and anticancer activities. The plant is rich in phytochemical constituents such as flavonoids furane, flavones, furanoflavonols, chromenoflavones, furanodiketones, flavonoid and glycosides ⁹. In the present study, the plant that was selected for synthesizing silver nanoparticles is *Aeschynomene aspera* L. (Niru-jilugu). The plant is an aquatic swampy herbal plant belonging to the family Fabaceae **Fig. 1** and **2**.



FIG. 1: AESCHYNOMENE ASPERA PLANT

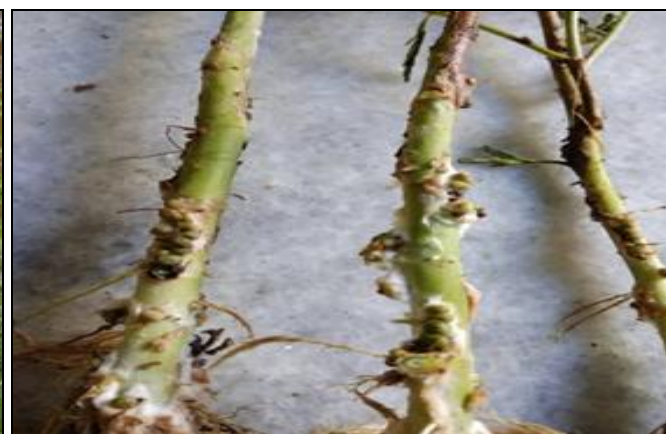


FIG. 2: AESCHYNOMENE ASPERA STEM NODULES

This plant, which is also known as Sola, Shola (Bengali), Sola pith plant (English), Laugauni (Hindi), Netti (Tamil) is commonly identified by nodular stems ¹⁰. *A. aspera* which is used as leafy vegetable possess medicinal values. It is generally used to cure urinary troubles but specifically in Siddha system, it is used to cure joint pains and swellings ¹¹. In Ayurveda system it is employed to break the painful kidney stones and calculi in the urinary tract ¹². The extracts of plant parts of *A. aspera* such as leaf, flower and fruits have been reported as rich source for phenols, alkaloids and tannins ¹⁰. Therefore, the present study was undertaken to synthesize and characterize the stable silver nanoparticles and validate its antimicrobial and antioxidant activities.

MATERIALS AND METHODS:

Plant Collection and Identification: The plant which grows abundantly in wet and wastelands during the rainy season (Oct-Dec) is common along margins of temporary water bodies. Plant material

of *A. aspera* specifically leaves were collected from Chavatapalem village along the water hedges near Chavitimadugu of Venkatachalam Mandal, Nellore District. The botanical identity of the plant was authenticated by Prof. N. Yasodamma. The voucher no. of *A. aspera* was VV 22 was deposited in the Herbarium, Sri Venkateswara University, Department of Botany, Tirupati.

Synthesis of Silver Nanoparticles [SNPs]: The leaves were initially washed with tap water and then washed with sterile distilled water to remove all the dust and unwanted visible particles. The leaves were cut into small pieces and dried at room temperature for 10 days to evaporate the residual moisture. The fine powder was obtained from dried leaves by using kitchen blender. 10g of powder was taken into a 250 ml conical flask and added 100 ml of Millie Q water and boiled for 30 min at 60 °C. The aqueous extract was separated by filtration with Whatman no. 1 filter paper and stored at room temperature for biosynthesis of silver nanoparticles

¹³. 2 mM AgNO₃ solution was prepared and stored in amber colour bottle. 10 ml of aqueous leaf extract was added to 90 ml of 2 mM silver nitrate (AgNO₃) solution (9:1 ratio). The reaction mixture was stirred for 10 min and incubated at room temperature. The colour of the resulting mixture was found to change from light yellow to dark brown within 1 h at room temperature indicating the formation of silver nanoparticles (AgNPs). The contents were centrifuged at 10,000 rpm at 25 °C for 10 min to remove the presence of biological admixtures from the supernatant and the resting AgNPs pellets were washed with double distilled water and then used for characterization, antimicrobial and antioxidant activities ¹⁴.

Characterization of Silver Nanoparticles:

Nanoparticles are generally characterized by their size, shape, surface area, and dispersity. The reduction of Ag⁺ to Ag⁰ done by the leaf extract was recorded by UV-visible spectroscopy (Nano drop-8000 spectrophotometer) between 200 to 800 nm. Dynamic light scattering (DLS) and Zeta potential of synthesized nanoparticles were analyzed to know the average size and stability of particles (Nanoparticle analyzer, Horiba SZ 100, Japan). The functional group of silver nanoparticles was identified by FT-IR (ALPHA interferometer, Bruker, Ettlingen, Karlsruhe, Germany) in the range of 4000-400 cm⁻¹ were recorded. The crystalline nature of AgNPs determined by XRD, powder X-ray diffraction patterns were recorded on a Bruker D8-Advance diffractometer using graphite monochromatic CuKα1 (1.5406 Å) radiations. The sample composition and elemental contents were analyzed by using an energy dispersive analysis system of X-ray (EDAX). The detailed morphology of synthesized AgNPs was investigated using High-Resolution Transmission Electron Microscopy (Model: FEI Tecnai, G² F20) with an acceleration voltage of 200kV at room temperature.

Antioxidant Activity [DPPH]: DPPH (2,2-diphenyl-1-picryl hydrazyl) free radical scavenging method involves the stock solution prepared by dissolving 4 mg of DPPH in 100 ml of methanol and stored at 20 °C. 2 ml of this solution was added to 1 ml of methanol solution containing test samples of *A. aspera* aqueous leaf extract and *A. aspera* leaf AgNPs at different concentrations (50-250 µg/ml). Ascorbic acid was used as a standard.

$$\text{RSA (\%)} = \frac{[Ac-As]}{Ac} \times 100$$

Where RSA is Radical scavenging activity, *Ac* is the absorbance of the control, and *As* is the absorbance of the sample or standard ¹⁵.

Antibacterial Activity: The antibacterial activity of biologically synthesized AgNPs of *A. aspera* leaf, aqueous and methanol extract were carried out against four bacterial strains. The antibacterial potential of the sample was assessed by following simple disc diffusion method. The antibacterial activity was tested on both Gram-positive and Gram-negative bacteria. For Gram-positive bacterial strains, *Bacillus subtilis* NCIM 2476, *Staphylococcus aureus* NCIM 2127, were used and for Gram-negative bacterial strains, *Pseudomonas aeruginosa* NCIM 5070, *Escherichia coli* NCIM 2068 were used. The method involved the spreading of overnight cultures of the respective organism onto nutrient agar medium plates. The samples were prepared by dissolving 1 mg dried powders of aqueous extracts, methanol extracts and AgNPs in 10 ml double distilled water. Ampicillin was taken as standard control and prepared by dissolving 25 µg in 10 ml double distilled water. The sterile discs of Whatman no. 1 filter paper of 5mm diameter were impregnated with 50 µl of each sample separately along with control and were placed at equal distance on the agar plates spread with respective bacteria. The agar plates were incubated at 37 °C for 24 h. The results were recorded after 24 h by measuring the diameter of the zone of inhibition in millimeters (mm) ¹⁶.

RESULTS:

UV-Vis Spectroscopy: The silver nanoparticles synthesized from aqueous leaf extract of *A. aspera* were initially confirmed by visual observation of color change within 20 min of the reaction mixture. The color change of the reaction mixture to completely dark brown was observed within 1 h of the incubation period. The appearance of a dark brown color was due to the excitation of nanoparticles Surface Plasmon Resonance (SPR). The UV-Vis spectrum showed maximum absorbance at 450 nm **Fig. 3**.

The presence of the secondary metabolites in leaf extract may be responsible for the reduction of silver and synthesis of nanoparticles.

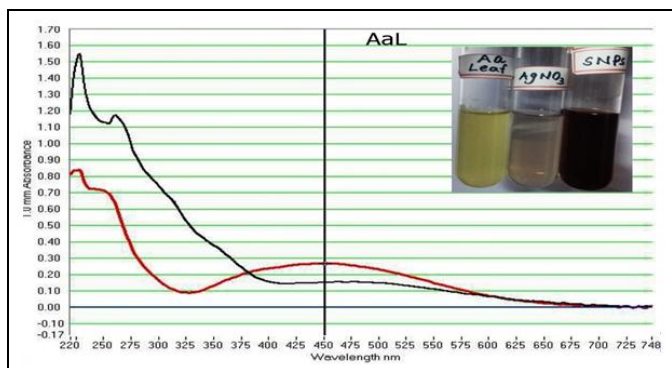


FIG. 3: UV-VIS SPECTROSCOPIC GRAPH SHOWING THE CHARACTERISTIC ABSORBANCE PEAK OF *A. ASPERA* LEAF AgNPs AT 450 nm. INSET PHOTOGRAPH INDICATES THE SYNTHESIS OF AgNPs

Dynamic Light Scattering (DLS) and Zeta Potential: Synthesized nanoparticles exhibited a polydispersed type of particles with 12 nm average mean size **Fig. 4a** and -15.8 mV of zeta potential value **Fig. 4b**. The polydispersity index of *A. aspera* leaf AgNPs shows 0.298, which indicates that the sample has a very narrow size distribution of nanoparticles. These outcomes reveal that the plant *A. aspera* leaf was a good source for the reduction of nano-size of AgNPs. The zeta potential value indicates synthesized nanoparticles have good stability in a liquid medium.

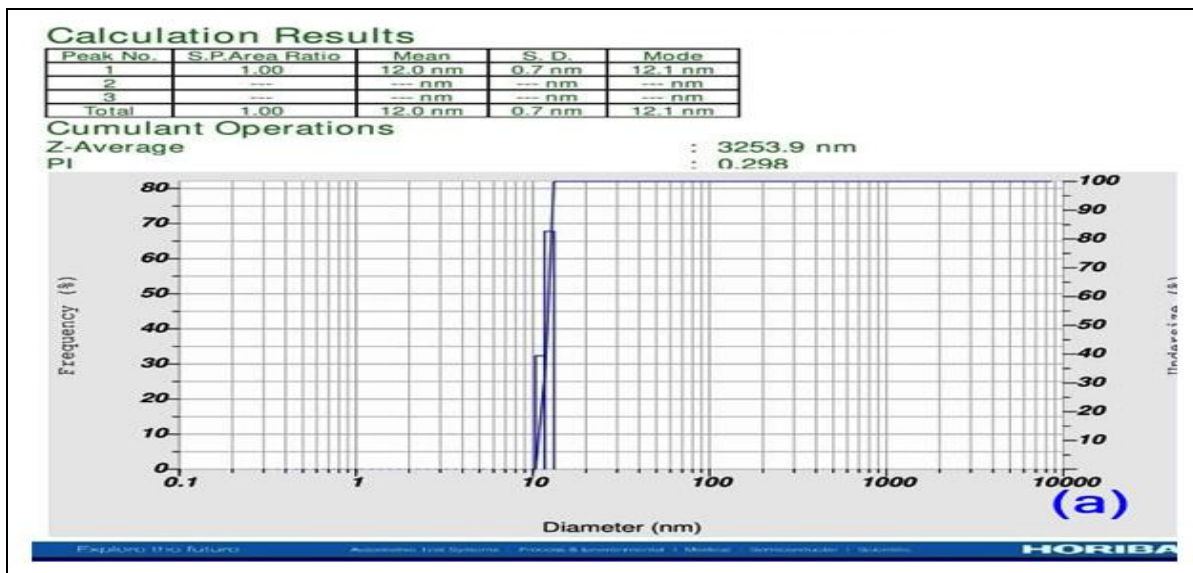


FIG. 4A: DLS: DYNAMIC LIGHT SCATTERING-MEAN AVERAGE SIZE AgNPs OF *A. ASPERA* LEAF

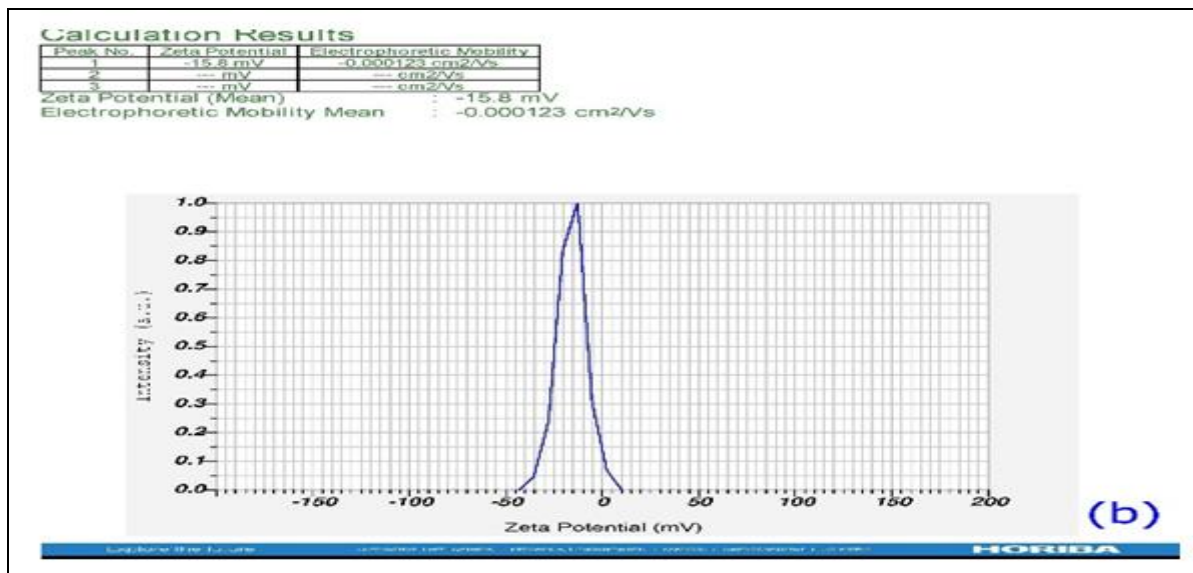


FIG. 4B: ZETA POTENTIAL ANALYSIS OF SYNTHESIZED AgNPs OF *A. ASPERA* LEAF

FT-IR Analysis: FT-IR absorption spectra of *A. aspera* leaf extract before and after the reduction of silver are shown in **Fig. 5** and **6**. The functional

group of *A. aspera* leaf extract was identified using FT-IR spectroscopy between the range from 641-3733 cm⁻¹ **Fig. 5**, **Table 1**. The FT-IR spectrum

displays a number of absorption peaks at 3733 & 3686 cm^{-1} with strong O-H molecule of water; 3546 O-H stretch free hydroxyl with functional group of alcohols; 3432 O-H stretch H-bonded alcohols/phenols; 3354(N-H stretch) amides; 3274 (O-H stretch) carboxylic acids; 3135 (C-triple bond-C-H stretch) alkynes group; 3019 (C=C)

alkenes; 2886 (C-H) alkanes; 2778,2709, 2602, 2531 (H-C=O) aldehydes; 2336, 2250, 2040 (C-H) aldehyde groups; 1691 (C=O) unsaturated ketones; 1545-nitro compounds N-H amide group; 1400-aromatic C-C stretch; 1097-(C-N) aliphatic amines; 959 (O-H bend) carboxylic acids; 841, 775, 714 alkyl halides; 641 alkynes.

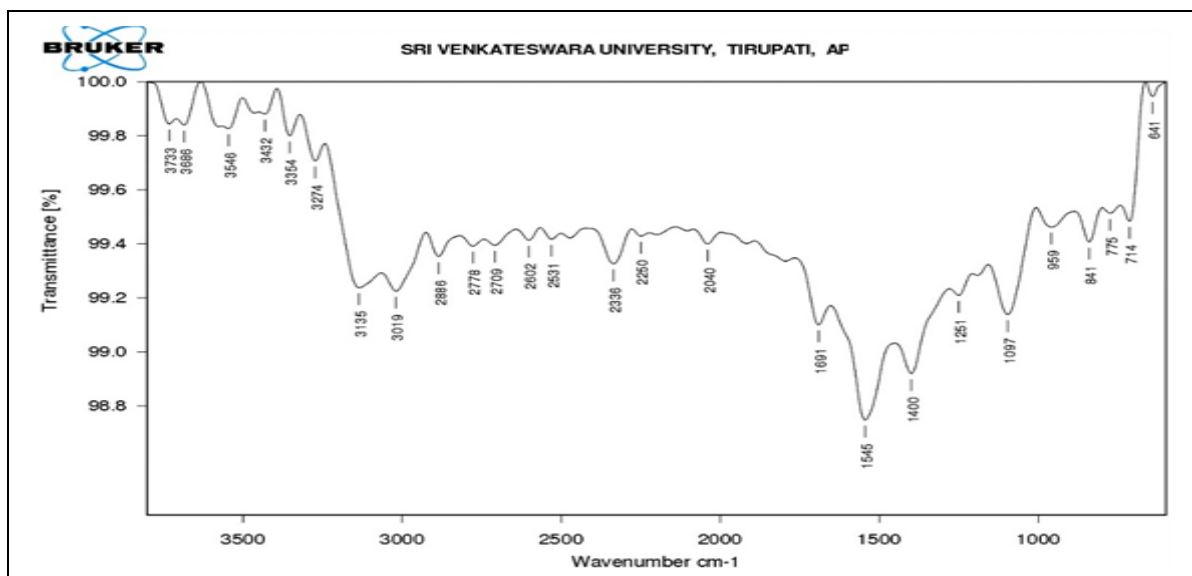


FIG. 5: FT-IR SPECTRUM USING AQUEOUS LEAF EXTRACT OF *A. ASPERA*

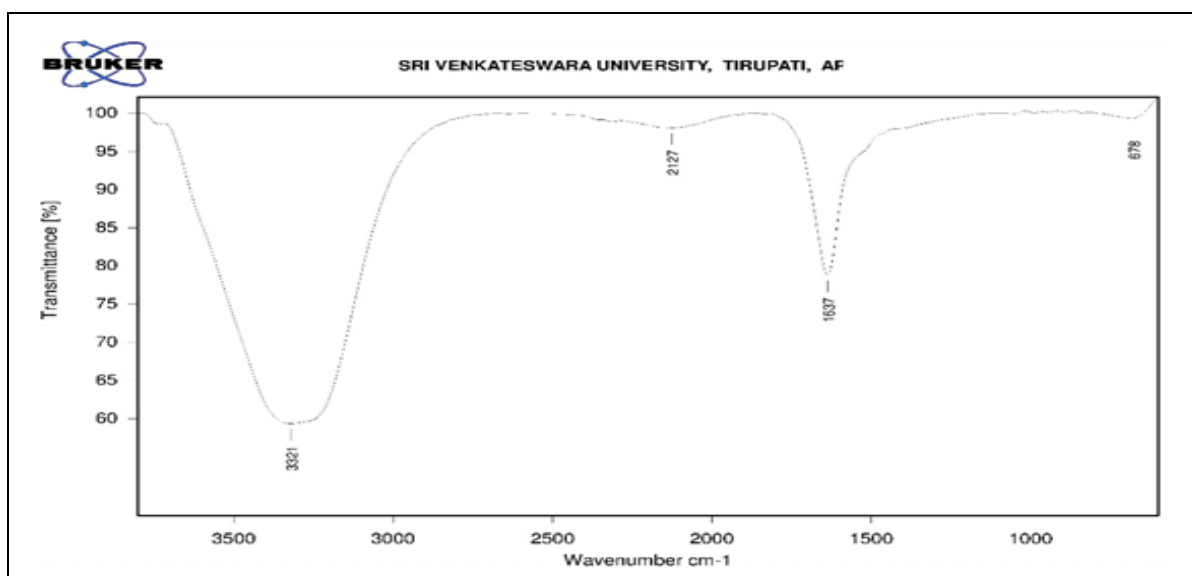


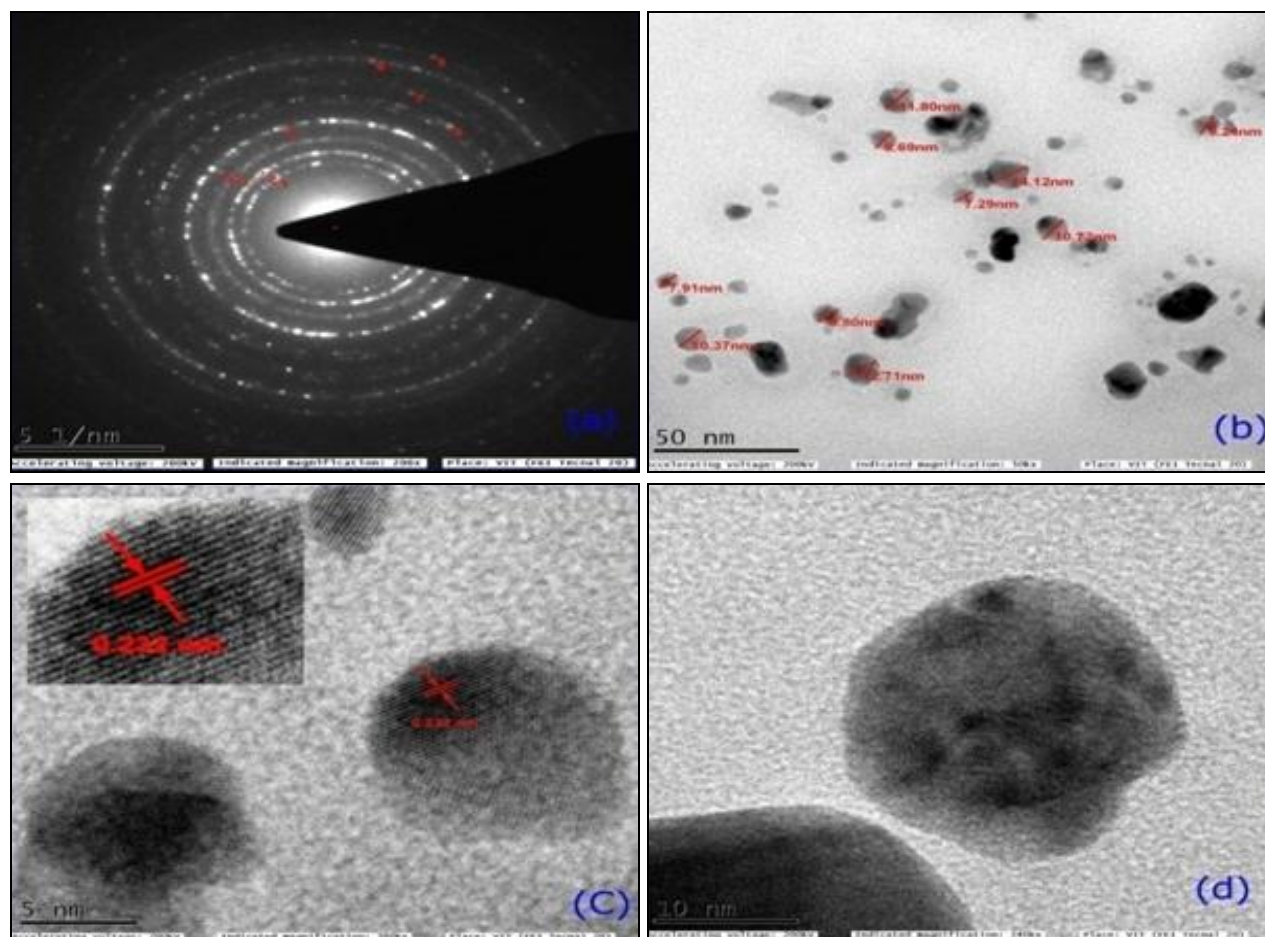
FIG. 6: FT-IR SPECTRUM OF SYNTHESIZED AgNPs USING AQUEOUS LEAF EXTRACT OF *A. ASPERA*

Biologically synthesized AgNPs of *A. aspera* leaf were identified using FT-IR spectroscopy at 678-3321 cm^{-1} range **Fig. 6**. The FT-IR spectrum obtained displays a number of absorption peaks like 3321 cm^{-1} assigned for O-H bond of alcohols/phenols; 2127 cm^{-1} monosubstituted C≡C triple bond alkyl groups; 1637 cm^{-1} can be attributed to C=O-NH₂ stretching probably due to the presence

of amide group and 678 cm^{-1} assigned for alkyl halides. Most of the peaks appeared in the *A. aspera* leaf extract was disappeared after synthesis of AgNPs **Fig. 6**. Based on FT-IR analysis it is confirmed that the broad peaks of phenols (3321 cm^{-1}) and amides (1637 cm^{-1}) are interacting with biosynthesized silver nanoparticles (AgNPs) and acting as a reducing agent.

TABLE 1: FT-IR ANALYSIS: IDENTIFIED FUNCTIONAL GROUPS FROM A. ASPERA LEAF AQUEOUS EXTRACT AND AgNPs

S. no.	Identified Frequency (cm ⁻¹) from A. aspera leaf aqueous extract	Functional group Stretch/bending	Identified functional group
1	3733 & 3686	O-H	Water
2	3546	O-H	Alcohols
3	3432	O-H	Alcohols/Phenols
4	3354	N-H	Amides
5	3274	O-H	Carboxylic acids
6	3135	C ≡ C	Alkynes group
7	3019	C=C	Alkenes
8	2886	C-H	Alkanes
9	2778,2709,2602 and 2531	H-C=O	Aldehydes
10	2336,2250 and 2040	C-H	Aldehyde groups
11	1691	C=O	Un saturated ketones
12	1545	N-H	Amide group
13	1400	C-C	Aromatic compounds
14	1097	C-N	Aliphatic amines
15	959	O-H	Carboxylic acids
16	841,775 and 714	C-H-X	Alkyl halides
17	641	C ≡ C	Alkynes
S. no.	Identified Frequency (cm ⁻¹) from A. aspera leaf AgNPs	Functional group Stretch/bending	Identified functional group
2	2127	C ≡ C	Mono substituted Alkyl groups
3	1637	C=O-NH ₂	Amide
4	678	C-H-X	Alkyl halides

**FIG. 7: HR-TEM IMAGES: (A) SELECTED AREA DIFFRACTION ANALYSIS (SAED), (B) 50 nm SCALE BAR IMAGE SHOWING NANOPARTICLES SIZES, (C) 5 nm SCALE BAR IMAGE-CALCULATION OF 'd' SPACE, (D) 10 nm SCALE BAR IMAGE- SPHERICAL SHAPED NANOPARTICLES**

HR-TEM Analysis: The HR-TEM images of synthesized leaf AgNPs of *A. aspera* **Fig. 7a, b, c & d** provide an indication regarding size, shape and distribution of nanoparticles. The selected area of electron diffraction (SAED) shows diffused rings. The crystalline (bright spots) and poly nanocrystalline (small spots) making up a ring. The 5nm resolution studies of nanoparticles showed a 0.232 nm size of 'd' space. This result indicates the synthesized nanoparticles were crystalline in nature. 50 nm scale bar studies signify that the synthesized nanoparticles are polydispersed and are spherical in shape, owing 7-11 nm size. No agglomerated AgNPs observed. The average sizes of nanoparticles were estimated as 10 nm in size. The DLS measured size is slightly higher when compared to the particle size measured from HR-TEM because DLS measures the hydrodynamic radius. The average size measured by DLS, HR-TEM and XRD showed nearly similar results in **Table 2**. The image **Fig. 7c** shows bright stripes called lattice fringes; they can appear in one to

other directions. If the image is very thin, these fringes can be interpreted as the projection of tunnels between columns of atoms, while dark lines are the atoms themselves. The 10 nm scale bar image **Fig. 7d** clearly shows that the nanoparticles are spherical in shape.

TABLE 2: AVERAGE SIZE MEASURED BY DLS, HR-TEM, AND XRD

DLS Analysis (nm)	HR-TEM (nm)	XRD (nm)
12	10	11.9

EDAX Analysis: The synthesized AgNPs of *A. aspera* leaf EDAX analysis confirmed the presence of strong silver 8.89% shows absorption peak at 3keV **Fig. 8** along with different elements and their weight percentages like carbon 81.02%, nitrogen 2.34%, and copper 7.75% **Table 3** without any contaminants. Metallic silver nanoparticles generally show a strong signal peak at 3keV, due to surface plasmon resonance. All the peaks of the silver are observed and assigned for Cu and C are derived from the carbon-coated copper.

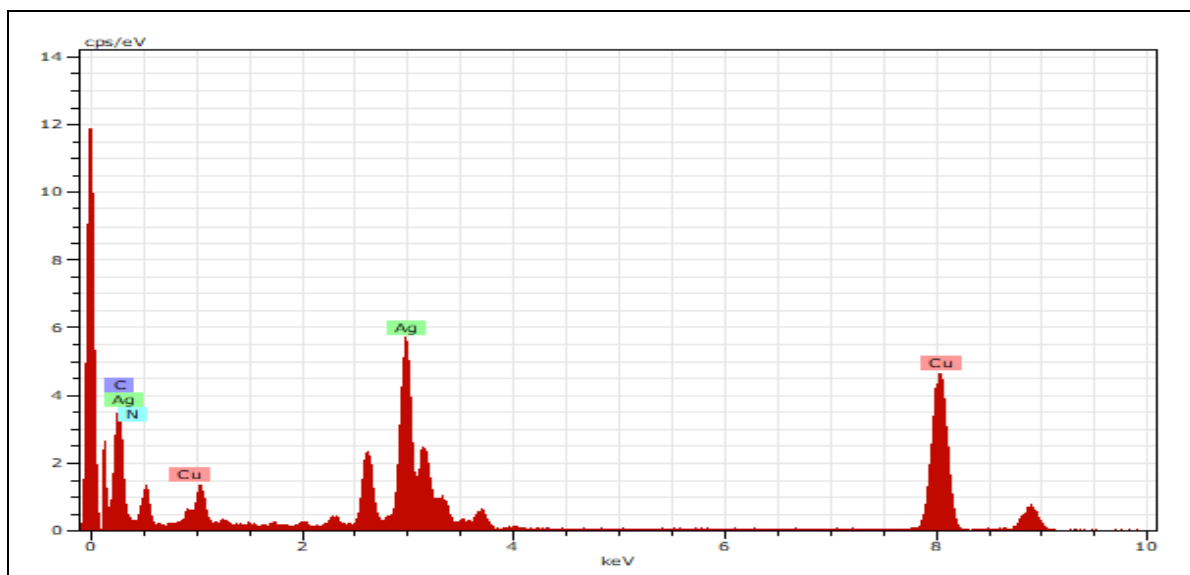


FIG. 8 EDAX SPECTRUM: AgNPs OF A. ASPERA LEAF

TABLE 3: EDAX SHOWS PERCENTAGE OF SILVER AND OTHER ELEMENTS IN SAMPLE

Element	Series	Net	Unn. C (wt. %)	Norm. C (wt. %)	Atom. C (at. %)	3 Sigma (wt. %)
Copper	K	23180	20.04	20.04	7.75	1.93
Silver	L	38036	39.02	39.02	8.89	11.80
Carbon	K	5836	39.61	39.61	81.02	3.96
Nitrogen	K	727	1.33	1.33	2.34	0.27
Total			100.00	100.00	100.00	

Unn. C = Unnormalised Concentration, Norm. C = Normalised Concentration, Atom. C = Atomic weight at percent, 3 Sigma = Weight percent concentration at 3 Sigma level.

XRD Analysis: The XRD results of the synthesized silver nanoparticles spectrum **Fig. 9** shows distinct diffraction peaks at $2\theta = 38.227^\circ$, 44.393° , 64.706° and 77.493° in the experimental

diffraction pattern have been identified to be due to silver metal and corresponding to hkl values (111), (200), (220) and (311) respectively **Table 4**. Thus, confirmed that the resultant particles in the prepared sample are silver nanoparticles having a face-centered cubic (fcc) crystal structure. The diffraction patterns have been compared with the standard powder diffraction card of JCPDS,

silver file no. 89-3722. In addition, two un-assigned peaks appeared at 32.450° and 46.533° which are weaker than those of silver. This may be due to the bio-organic compounds occurring on the surface of the AgNPs. The average crystalline size D of the silver nanoparticles have been estimated from the diffraction pattern by using Debye-Scherrer formula ($D = K\lambda/\beta \cos \theta$)

TABLE 4: XRD RESULTS OF SILVER NANOPARTICLES OF A. ASPERA LEAF

S. no.	2θ ($^\circ$)	COS θ	FWHM 2θ ($^\circ$)	d-spacing (\AA)	Crystalline Size 'D' nm	h k l Identified from peak	$h^2+k^2+l^2$ from identified hkl
1	38.227	0.7855	0.524	2.35246	16.7	111	3
2	44.393	0.7145	1.294	2.03899	6.93	200	4
3	64.706	0.4272	0.639	1.43942	15.3	220	8
4	77.493	0.2165	1.241	1.23075	8.5	311	11

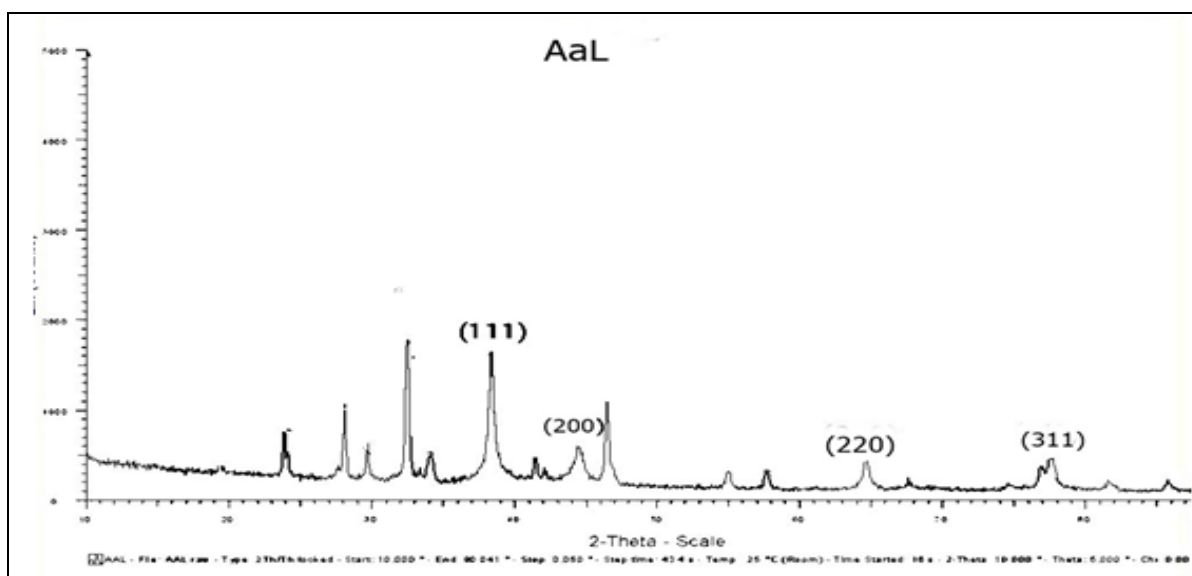


FIG. 9: XRD PATTERNS OF SYNTHESIZED AgNPs USING AQUEOUS LEAF EXTRACT OF A. ASPERA

DPPH Method of Antioxidant Analysis: The aqueous leaf extract and synthesized AgNPs of *A. aspera* showed better antioxidant potential when compared to standard ascorbic acid by DPPH scavenging assay method. Different concentrations ranging from 50-250 $\mu\text{g/ml}$ of *A. aspera* leaf aqueous extract and *A. aspera* AgNPs; Ascorbic acid was taken as a positive control to compare the percentage activity of the aqueous leaf extract and silver nanoparticles **Fig. 10**. The antioxidant

activity observed was increased in dose-dependent manner. The highest percentage activity was exhibited at 250 $\mu\text{g/ml}$ *A. aspera* leaf extract (56.22) < *A. aspera* leaf AgNPs (67.48) < Ascorbic acid (72.26) **Table 5**. From the results, it is concluded that silver nanoparticles of *A. aspera* leaf extract possess good DPPH activity when compared to that of leaf extract alone. The antioxidant activity of AgNPs by the DPPH method shows a strong absorption band at 517 nm.

TABLE 5: DPPH ANTIOXIDANT ACTIVITY A. ASPERA LEAF EXTRACT AND A. ASPERA-AgNPs

Concentration ($\mu\text{g/ml}$)	<i>A. aspera</i> leaf extract (% activity)	<i>A. aspera</i> AgNPs (% activity)	Ascorbic acid (% activity)
50	18.72	33.16	42.27 ± 0.26
100	32.64	42.86	52.43 ± 0.07
150	45.70	56.14	61.44 ± 0.56
200	47.12	59.08	66.54 ± 0.67
250	56.22	67.48	72.26 ± 0.67

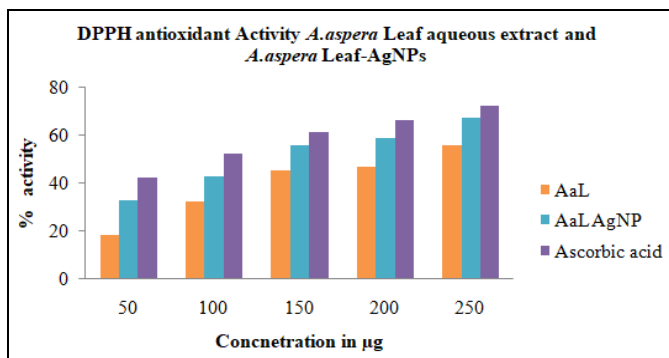


FIG. 10: DPPH RADICAL SCAVENGING ASSAY: ANTIOXIDANT EFFICACY BAR GRAPH OF A. ASPERA LEAF AQUEOUS EXTRACT, AgNPs, AND ASCORBIC ACID

Antibacterial Activity: The biologically synthesized AgNPs of *A. aspera* showed excellent antibacterial activity against the bacterial pathogens

B. subtilis, *E. coli*, *S. aureus*, *P. aeruginosa*. The zone of inhibition of AgNPs was observed in *E. coli* 14.1 mm and *P. aeruginosa* 12.2 mm followed by *S. aureus* 11.3 mm, *B. subtilis* 11.1 mm at 50 µl concentrations when compared to Ampicillin as standard **Fig. 11; Table 6**. The zone of inhibition of methanol extract on *E. coli* 12.2 mm on *P. aeruginosa* 10.7 mm followed by *B. subtilis* 10.4 mm and *S. aureus* 10.2 mm. The aqueous and methanol leaf extracts of *A. aspera* showed a limited zone of inhibition compared to AgNPs. The above result clearly showed that the synthesized AgNPs have potent antibacterial activity against Gram-negative bacteria compared to Gram-positive bacteria.

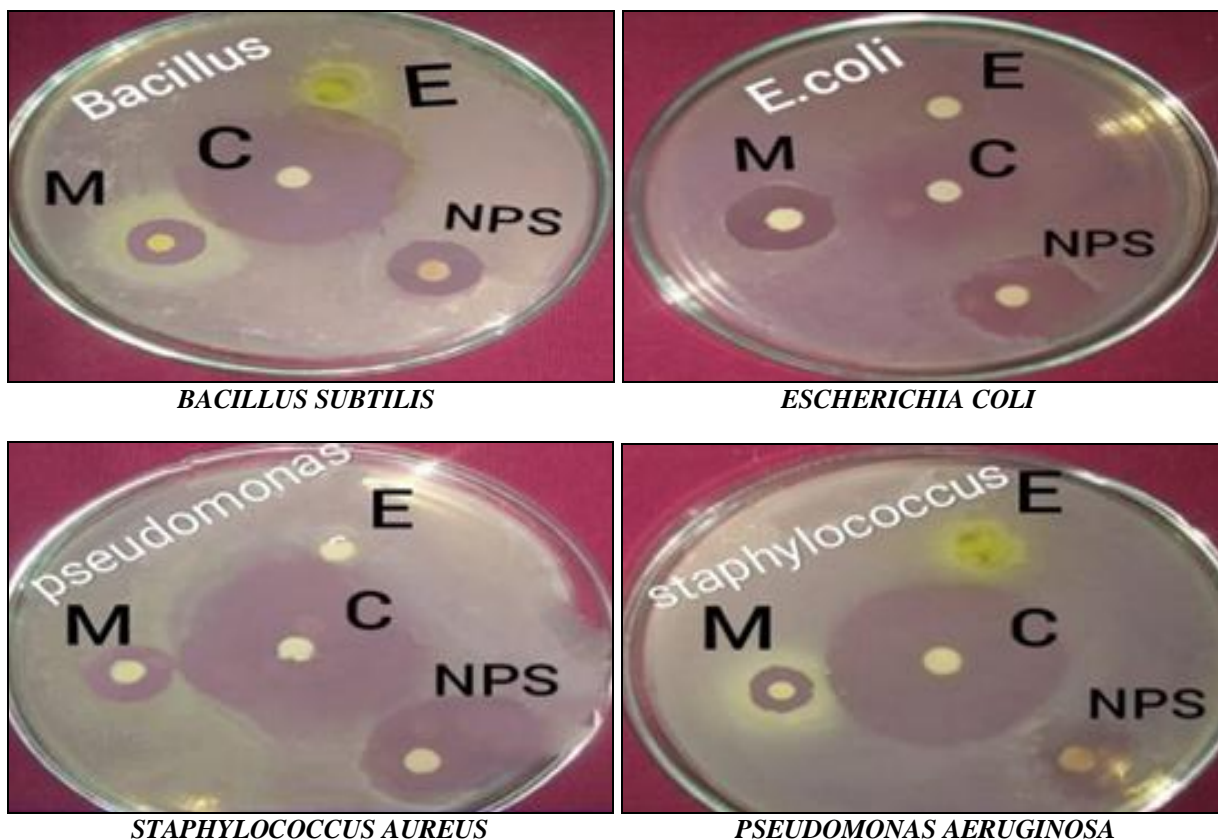


FIG. 11: ANTIBACTERIAL ACTIVITY OF A. ASPERA LEAF AQUEOUS EXTRACT, METHANOL EXTRACT AND AgNPs AGAINST DIFFERENT BACTERIAL STRAINS

TABLE 6: ANTIBACTERIAL ACTIVITY OF DIFFERENT STRAINS OF BACTERIA AND THEIR ZONE OF INHIBITION IN ‘mm’

Sample/Test organism	<i>Bacillus subtilis</i>	<i>E. coli</i>	<i>Staphylococcus aureus</i>	<i>Pseudomonas aeruginosa</i>
AaLE	8.2 ± 0.21**	—	5.2 ± 0.55**	—
AaLM	10.4 ± 0.19**	12.2 ± 0.11**	10.2 ± 0.19**	10.7 ± 0.16**
AaL NPs	11.1 ± 0.12**	14.1 ± 0.09**	11.3 ± 0.08**	12.2 ± 0.19**
Control Ampicillin	20.3 ± 0.11	17.6 ± 0.07	25.0 ± 0.57	27.1 ± 0.17

E- Aqueous extract; M-Methanol; C- Control; NPs- AgNPs. All the data are expressed as mean ±SEM: ***p*<0.01, **p*<0.05 as compared to control group, n=4: (One –way ANOVA followed by Dunnett’s test).

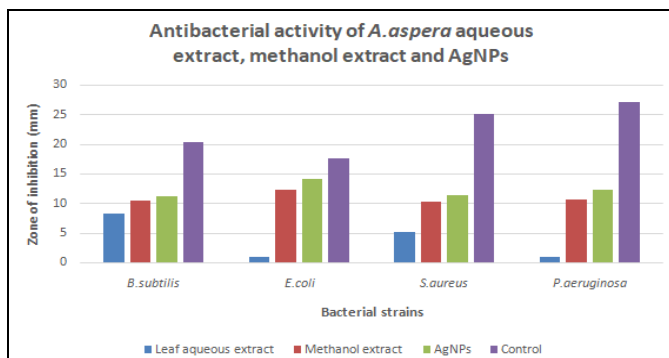


FIG. 12: ZONE OF INHIBITION OF DIFFERENT EXTRACTS OF A. ASPERA ON BACTERIAL STRAINS

DISCUSSION: Several studies have reported the successful synthesis of nanoparticles with Fabaceae family members. The silver nanoparticles have been synthesized by using extracts from the different plant parts but most specifically with leaf extracts. Although, the reaction times for the synthesis of silver nanoparticles varied for different plants but the particles are formed successfully. For example, silver nanoparticles of *Cicer arietinum* and *Pongamia pinnata* were synthesized in one hour, *Abrus precatorius* nanoparticles were synthesized after 5 min, *Calliandra haematocephala* nanoparticles were formed after 10 min, *Butea monosperma* SNPs were synthesized after 24 h of incubation whereas *Aeschynomene aspera* nanoparticles were synthesized in 1 h incubation period. The formation of silver nanoparticles was confirmed by observing the absorption peak. Earlier reports showed the absorption peaks for example, *Cicer arietinum* at 418 nm, *Abrus precatorius* in the range of 320 nm to 400 nm, *Calliandra haematocephala* at 414nm, *Butea monosperma* showed the peak at 400nm and *Aeschynomene aspera* showed the absorption peak at 451 nm.

This clearly shows that the absorption peaks were observed in the range of 320 nm to 450 nm. The morphology of the nanoparticles was measured by employing different techniques such as TEM, SEM and AFM. SEM micrographs of *Cicer arietinum* showed the morphology of nanoparticles as spherical in shape, with 40-60 nm size, *Abrus precatorius* particles appeared as disk-shaped with an average size between 35-40 nm, *Pongamia pinnata* appeared as spherical in shape with particle size of 5-55 nm and *Aeschynomene aspera* particles appeared as spherical in shape with 10 to 12 nm in size.

The functional groups of the silver nanoparticles prepared from the extracts were analyzed by using FT-IR spectrums. The FT-IR spectrum clearly shows the interactions of silver nanoparticles with the functional compounds present in the extract. The FT-IR analysis of *C. arietinum* particles revealed the presence of primary amines, carbonyl group ketone, aldehydes, and hydroxyl group carboxylic acids, alcohol and phenols as main compounds⁵. *A. precatorius* FTIR spectrum showed the interaction of the amide bond carbonyl proteins, alcohols and phenolic compounds with Ag nanoparticles⁶. *C. haematocephala* FT-IR spectrum revealed the presence of hydrogen-bonded alcohol and phenols⁸.

In the present study, FT-IR analysis of *A. aspera* extracts showed the presence of different types of functional molecules but phenols and amides were interacting with the silver nanoparticles.

The experimental analysis of the bioactive compounds existing in the leaf extracts of *A. aspera* showed the presence of major secondary metabolites such as flavonoids group of flavones, phenolic compounds, terpenoids and saponins. Further qualitative analysis of phenolic compounds revealed the presence of caffeic acid, phloroglucinol, β -resorcylic acid, neo-chlorogenic acid, Homo-protocatechnic acid, Trans-sinapic acid and cinnamic acid. Qualitative analysis of flavonoid compounds revealed the presence of myricetin, quercetin and apigenin¹⁰.

The phytochemicals present in the *A. aspera* extracts exhibit different therapeutic functions. Compounds such as caffeic acid show antibacterial, antioxidant, antidiabetic, anti-inflammatory, anti-carcinogenous, antiproliferative, hepatoprotective and cardioprotective function¹⁷⁻²¹, protocatechuic acid acts as inflammatory²², chlorogenic acid act as anticancer^{23, 24}. Also, include sinapic acid which acts as antioxidant²⁵, cinnamic acid acts as anticancer, antioxidant^{26, 27}, coumaric acid acts as antibacterial, immunomodulatory, antioxidant activity²⁸⁻³¹. Flavonoid compounds such as myricetin show anti-atherosclerotic show, anti-inflammatory^{32, 33}, Apigenin acts as antioxidant, anti-hyperglycaemic, anti-inflammatory, anti-apoptotic, cytotoxic, cardiovascular³⁴⁻³⁹. Quercetin acts as antiatherosclerotic⁴⁰.

The antibacterial activity of Fabaceae family members was reported earlier. Silver nanoparticles of *C. arietinum* showed antibacterial activity against *E. coli*. The activity was equal to the activity of standard drugs Rifampicin, Cefimex and Ampicillin⁵. Although, some of the plant extracts exhibited antibacterial activity against both Gram-positive and Gram-negative bacteria, but the effect of the action is different. Antibacterial activity of *A. precatorius* silver nanoparticles on *P. aeruginosa* showed maximum zone of inhibition as 24 mm⁶. AgNPs of *C. ternatea* showed a strong inhibitory action against *P. aeruginosa* along with *S. aureus*, *E. coli* and *S. viridi*⁷. AgNPs of *C. haematocephala* showed effective antibacterial activity against *E. coli*⁸.

In the present study, the AgNPs of *A. aspera* showed antibacterial activity against all selected four bacterial strains with an average of 22.4 mm to 29.0 mm diameter zone of inhibition which is twice to that of control drug activity.

CONCLUSION: In the present study, the leaf extracts of *A. aspera* were used as a source for synthesizing the silver nanoparticles. By using the traditional procedures, the AgNPs were prepared. The confirmation of AgNPs synthesis has come initially by the observation of color change and then by observing the peak at 450 nm in the UV-Vis absorption spectra. DLS analysis revealed 12 nm average mean sizes and Zeta potential analysis revealed -15.8 mV of negative Zeta potential value which indicates nanoparticles stability. The FT-IR spectrum revealed the presence of various functional groups like alcohol/phenols, alkyl, amide, alkyl halides groups which are responsible for the reduction of Ag⁺ ions to Ag. HR-TEM image reveals that the nanoparticles are spherical in shape with a size range from 7-11 nm. The average size of the nanoparticles was 10 nm. These particles are in a poly-dispersed condition. The crystalline structure and 11.9 nm average size of the particles were revealed by XRD analysis. Based on the analysis of DLS, HR-TEM and XRD, it was confirmed that the average size of synthesized silver nanoparticles of *A. aspera* was less than 20 nm. The presence of silver and other elements was confirmed by EDAX analysis. The biosynthesized AgNPs showed potent antioxidant activity with a value of 67.48%.

In the present study, the silver nanoparticles prepared from the leaf extracts of *A. aspera* appeared as very small *i.e.* 10 nm sizes when compared with nanoparticles prepared from other plants of the same family. If the antibacterial activity is compared with other plants, the silver nanoparticles prepared from *A. aspera* exhibited a tremendous activity. The extracts have shown an average of 22.4mm to 29.0mm zone of inhibition which is double to that of the control used. Based on the antibacterial activity, it is likely to assign the AgNPs of *A. aspera* as anticonjunctivities, wound healer, antidiarrhoeal, anticolitis, against gastroenteritis and to cure urinary tract infections as the extracts were effective against *E. coli*, *B. subtilis* and *S. aureus*.

Overall, the characterization of silver nanoparticles from the leaf extracts of *A. aspera* and evaluation of its antimicrobial and antioxidant activities of the SNPs recommend their application in the pharmaceutical industry for designing drugs against tumors and bacterial infections.

ACKNOWLEDGEMENT: We are indebted to the Department of Botany, S.V.U College of Sciences, Sri Venkateswara University, Tirupati, Andhra Pradesh, India for providing the space and facilities to complete the above Research work. We are also extending acknowledgements to the RRSFP program, DBT, S. V. U, Tirupati, for assistance in the completion of the research work.

CONFLICTS OF INTEREST: There is no conflict of interest related to this work by any of the authors.

REFERENCES:

1. Ahmed S, Ahmad M, Swami BL and Ikram S: A review on plants extract mediated synthesis of silver nanoparticles for antimicrobial applications: A green expertise. Journal of Advanced Research 2016; 7(1): 17-28.
2. Lopes CRB and Courrol LC: Green synthesis of silver nanoparticles with extract of *Mimusops coriacea* and light. Journal of Luminescence 2018; 199: 183-7.
3. Bendale Y, Bendale V and Paul S: Evaluation of cytotoxic activity of platinum nanoparticles against normal and cancer cells and its anticancer potential through induction of apoptosis. Integrative Medicine Research 2017; 6(2): 141-8.
4. Dzoyem JP, McGaw LJ and El JN: *In-vitro* antibacterial, antioxidant and cytotoxic activity of acetone leaf extracts of nine under-investigated Fabaceae tree species leads to potentially useful extracts in animal health and

- productivity. BMC Complementary and Alternative Medicine 2014; 14: 147.
5. Agarwal R, Kumar N and Singh R: *Cicer arietinum* leaf extract mediated synthesis of silver nanoparticles and screening of its antimicrobial activity. Adv Sci Med 2014; 6: 1-5.
 6. Gaddala B and Nataru S: Synthesis, Characterization and evaluation of silver nanoparticles through leaves of *Abrus precatorius* L. an important medical plant. Appl Nanosci 2015; 5(1): 99-104.
 7. Krithiga N, Rajalakshmi A and Jayachitra A: Green synthesis of silver nanoparticles using leaf extracts of *Clitoria ternatea* and *Solanum nigrum* and study of its antibacterial effect against common nosocomial pathogens. Journal of Nanoscience 2015; 1-8.
 8. Raja S, Ramesh V and Thivaharan V: Green biosynthesis of silver nanoparticles using *Calliandra haematocephala* leaf extract, their antibacterial activity and hydrogen peroxide sensing capability. Arabian Journal of Chemistry 2017; 10(2): 253-61.
 9. Rajeshkumar S: Synthesis of silver nanoparticles using fresh bark of *Pongamia pinnata* and characterization of its antibacterial activity against gram positive and gram-negative pathogens. Resource-Efficient Technologies 2016; 2(1): 30-35.
 10. Aruna C, Suvarnalatha A, Chaithra D, Alehkya C, Yasodamma N and Meerasahib C: Phytochemical and antimicrobial studies of a herbal medicinal plant *Aeschynomene aspera* L. leaf extract. Journal of Pharmacy Research 2013; 5(4): 1827-37.
 11. Muralidhar CSM and Vaguppu GM: 4th Edition, Tamil Nadu Siddha Medicinal Council; Chennai 1988; 1-680.
 12. Rajan G, Bhaskar, Alikhan I and Khanum A: Strength and wealth of therapeutic medicinal plants in India, Published in Irfan Khan and Atiya Khanum (Eds). Uttaz Publications 2004; 1(8): 286-93.
 13. Shankar SS, Rai A, Ankamwar B, Singh A, Ahmad A and Sastry M: Biological synthesis of triangular gold nanoparticles. Nature Materials 2004; 3(7): 482.
 14. Saifuddin N, Wong CW and Yasumira AA: Rapid biosynthesis of silver nanoparticles using culture supernatant of bacteria with microwave irradiation, Journal of Chemistry 2009; 6(1): 61-70.
 15. Sharma OP and Bhat TK: DPPH antioxidant assay revisited, Food Chemistry 2009; 113(4): 1202-05.
 16. Bauer AW, Kirby WMM, Sherris JC and Turck M: Antibiotic susceptibility testing by a standardized single disk method, American Journal of Clinical Pathology 1966; 45(4): 493-96.
 17. Genaro-Mattos TC, Maurício ÂQ, Rettori D, Alonso A and Hermes-Lima M: Antioxidant activity of caffeic acid against iron-induced free radical generation-A chemical approach. PLoS ONE 2015; 10(6): e0129963.
 18. Tosovic J: Spectroscopic features of caffeic acid: theoretical study. Kragujev J Sci 2017; 39: 99-108.
 19. Rodrigues JL, Araújo RG, Prather KLJ, Kluskens LD and Rodrigues LR: Heterologous production of caffeic acid from tyrosine in *Escherichia coli*. Enzyme and Microb Tech 2015; 71: 36-44.
 20. Xie J, Yang F, Zhang M, Lam C, Qiao Y and Xiao J: Antiproliferative activity and SARs of caffeic acid esters with mono-substituted phenylethanols moiety. Bioorg Med Chem Lett 2017; 27: 131-34.
 21. Bispo VS, Dantas LS, Chaves Filho AB, Pinto IFD, Silva Rp DA and Otsuka FAM: Reduction of the DNA damages, hepatoprotective effect and antioxidant potential of the coconut water, ascorbic and caffeic acids in oxidative stress mediated by ethanol. An Acad Bras Cienc 2017; 89: 1095-9.
 22. Peiffer DS, Zimmerman NP and Wang LS: Chemoprevention of esophageal cancer with black raspberries, their component anthocyanins, and a major anthocyanin metabolite, protocatechuic acid. Cancer Prevention Research 2014; 7(6): 574-84.
 23. Maalik A, Bukhari SM, Zaidi A, Shah KH and Khan FA: Chlorogenic acid: a pharmacologically potent molecule. Acta Poloniae Pharmaceutica 2016; 74: 851-54.
 24. Yamagata K, Izawa Y, Onodera D and Tagami M: Chlorogenic acid regulates apoptosis and stem cell marker-related gene expression in A549 human lung cancer cells. Mol Cell Biochem 2018; 441(1-2): 9-19.
 25. Chen C: Sinapic acid and its derivatives as medicine in oxidative stress-induced diseases and aging. Oxid Med Cell Longev 2016; 4: 1-10.
 26. Kopp C, Singh SP, Regenhard P, Müller U, Sauerwein H and Mielenz M: Trans-cinnamic acid increases adiponectin and the phosphorylation of AMP-activated protein kinase through g-protein-coupled receptor signaling in 3T3-L1 adipocytes. International Journal of Molecular Sciences 2014; 15(2): 2906-15.
 27. Li W, Zhao X, Sun X, Zu Y, Liu Y and Ge Y: Evaluation of antioxidant ability *in-vitro* and bioavailability of trans-cinnamic acid nanoparticle by liquid antisolvent precipitate. Journal of Nanomaterials 2016; 10: 1-11.
 28. Guven M, Yuksel Y, Sehitoğlu MH, Tokmak M, Aras AB and Akman T: The effect of coumaric acid on ischemia-reperfusion injury of sciatic nerve in rats. Inflammation 2015; 38: 2124-32.
 29. Thakur K, Kalia S, Sharma N and Pathania D: Laccase-mediated biografting of p-coumaric acid for development of antibacterial and hydrophobic properties in coconut fibers. J Mol Catal B Enzym 2015; 122: 289-95.
 30. Akkoyun HT and Karadeniz A: Investigation of the protective effect of ellagic acid for preventing kidney injury in rats exposed to nicotine during the fetal period. Biotech Histochem 2016; 91: 108-15.
 31. Kilani-Jaziri S, Mokdad-Bzeouich I, Krifa M, Nasr N, Ghedira K and Chekir-Ghedira L: Immunomodulatory and cellular antioxidant activities of caffeic ferulic and p-coumaric phenolic acids: a structure-activity relationship study. Drug Chem Toxicol 2016; 18: 1-9.
 32. Liu S, Ai Q, Feng K, Li Y and Liu X: The cardioprotective effect of dihydromyricetin prevents ischemia-reperfusion-induced apoptosis *in-vivo* and *in-vitro* via the PI3K/Akt and HIF-1 α signaling pathways. Apoptosis 2016; 21: 1366-85.
 33. Liu TT, Zeng Y, Tang K, Chen X, Zhang W and Xu XL: Dihydromyricetin ameliorates atherosclerosis in LDL receptor deficient mice. Atherosclerosis 2017; 262: 39-50.
 34. Fidelis QC, Faraone I, Russo D, Catunda FEA, Vignola LJ, de Carvalho MG, de Tommasi N and Milella L: Chemical and Biological insights of *Ouratea hexasperma* (A. St.-Hil.) Baill.: A source of bioactive compounds with multifunctional properties. Nat Prod Res 2018; 1-4.
 35. Villa-Rodriguez JA, Kerimi A, Abranko L, Tumova S, Ford L, Blackburn RS, Rayner C and Williamson G: Acute metabolic actions of the major polyphenols in chamomile: An *in-vitro* mechanistic study on their potential to attenuate postprandial hyperglycaemia. Sci Rep 2018; 3: 5471.
 36. Zhou Z, Zhang Y, Lin L and Zhou J: Apigenin suppresses the apoptosis of H9C2 rat cardiomyocytes subjected to myocardial ischemia-reperfusion injury *via* upregulation of the PI3K/Akt pathway. Mol Med Rep 2018; 18: 1560-70.

37. Zhou X, Wang F, Zhou R, Song X and Xie M: Apigenin: A current review on its beneficial biological activities. J. Food Biochem 2017; 41: e12376.
38. Pereira SV, Reis RASP, Garbuio DC and de Freitas LAP: Dynamic maceration of *Matricaria chamomilla* inflorescences: Optimal conditions for flavonoids and antioxidant activity. Rev Bras Farmacog 2018; 28: 111-17.
39. Zainal-Abidin MH, Hayyan M, Hayyan A and Jayakumar NS: New horizons in the extraction of bioactive compounds using deep eutectic solvents: A review. Anal. Chim. Acta 2017; 979: 1-23.
40. Salvamani S, Gunasekaran B, Shaharuddin NA, Ahmad SA and Shukor MY: Antiatherosclerotic effects of plant flavonoids. Biomed Res Int 2014; 10: 1-11.

How to cite this article:

Vishnuvardhan K, Bommana K and Nimmanapalli Y: Phytochemical screening, silver nanoparticle synthesis and antibacterial studies on the leaves of *Aeschynomene aspera* L. Int J Pharm Sci & Res 2020; 11(1): 451-63. doi: 10.13040/IJPSR.0975-8232.11(1).451-63.

All © 2013 are reserved by the International Journal of Pharmaceutical Sciences and Research. This Journal licensed under a Creative Commons Attribution-NonCommercial-ShareAlike 3.0 Unported License.

This article can be downloaded to **Android OS** based mobile. Scan QR Code using Code/Bar Scanner from your mobile. (Scanners are available on Google Play store)